World Academy of Science, Engineering and Technology
International Journal of Civil and Environmental Engineering
Vol:11, No:9, 2017

Prediction of Time to Crack Reinforced Concrete by Chloride Induced Corrosion

Anuruddha Jayasuriya, Thanakorn Pheeraphan

Open Science Index, Civil and Environmental Engineering Vol:11, No:9, 2017 publications.waset.org/10007834/pdf

***Abstract*—**In this paper, a review of different mathematical models which can be used as prediction tools to assess the time to crack reinforced concrete (RC) due to corrosion is investigated. This investigation leads to an experimental study to validate a selected prediction model. Most of these mathematical models depend upon the mechanical behaviors, chemical behaviors, electrochemical behaviors or geometric aspects of the RC members during a corrosion process. The experimental program is designed to verify the accuracy of a well-selected mathematical model from a rigorous literature study. Fundamentally, the experimental program exemplifies both one-dimensional chloride diffusion using RC squared slab elements of 500 mm by 500 mm and two-dimensional chloride diffusion using RC squared column elements of 225 mm by 225 mm by 500 mm. Each set consists of three water-to-cement ratios (w/c); 0.4, 0.5, 0.6 and two cover depths; 25 mm and 50 mm. 12 mm bars are used for column elements and 16 mm bars are used for slab elements. All the samples are subjected to accelerated chloride corrosion in a chloride bath of 5% (w/w) sodium chloride (NaCl) solution. Based on a pre-screening of different models, it is clear that the well-selected mathematical model had included mechanical properties, chemical and electrochemical properties, nature of corrosion whether it is accelerated or natural, and the amount of porous area that rust products can accommodate before exerting expansive pressure on the surrounding concrete. The experimental results have shown that the selected model for both one-dimensional and two-dimensional chloride diffusion had ±20% and ±10% respective accuracies compared to the experimental output. The half-cell potential readings are also used to see the corrosion probability, and experimental results have shown that the mass loss is proportional to the negative half-cell potential readings that are obtained. Additionally, a statistical analysis is carried out in order to determine the most influential factor that affects the time to corrode the reinforcement in the concrete due to chloride diffusion. The factors considered for this analysis are w/c, bar diameter, and cover depth. The analysis is accomplished by using Minitab statistical software, and it showed that cover depth is the significant effect on the time to crack the concrete from chloride induced corrosion than other factors considered. Thus, the time predictions can be illustrated through the selected mathematical model as it covers a wide range of factors affecting the corrosion process, and it can be used to predetermine the durability concern of RC structures that are vulnerable to chloride exposure. And eventually, it is further concluded that cover thickness plays a vital role in durability in terms of chloride diffusion.

***Keywords*—**Accelerated corrosion, chloride diffusion, corrosion cracks, passivation layer, reinforcement corrosion.

Anuruddha Jayasuriya was a former graduate student with the Asian Institute of Technology, (AIT) Thailand (e-mail: ajayasuriya77@ gmail.com).

Thanakorn Pheeraphan is with the Navaminda Kasatriyadhiraj Royal Air Force Academy, and AIT Thailand (e-mail: petevmi91@yahoo.com).

I. Introduction

CORROSION is one of the prominent causes of deterioration of concrete structures in North America. Concrete indeed a hardened cement paste that contains a high pH range around 12.5 to 13.5 due to its rich alkalinity [18]. But however, this alkalinity can be reduced due to the breakage of the passivation layer around the steel. This de-passivation can be due to chloride ion adsorption, repulsion of chloride ion due to its negative charge, and reaction of chloride with Fe_2O_3 which exists already around the steel rebar as a protective passivation layer [6], [7], [10], [11], [23]. The disruption of the passivation layer can lead to initiate corrosion and exert expansive stresses on the surrounding concrete. Many mathematical models have been developed over the years to predict the time to crack the concrete (T_{cr}) due to corrosion [4], [5], [9], [13], [19], [20], [27]. The accuracies of such models predominantly depend on the factors that are being considered.

A thorough literature review on prediction models is conducted. However, since corrosion is so far understood as an electrochemical process, most of the models are incorporated with chemical and electrochemical properties [2], [21], [22]. In addition, the mechanical properties, concrete porosity and the structural geometries have also been used in some time prediction models [9]-[12].

II. Methodology

A. Preliminary Study-Pre-Screening Stage

Many models discuss about considering different influential factors for the T_{cr} due to corrosion. However, an accuracy check is done based on the available data as a preliminary study for this research. Table I shows a summary on comparison of experimental T_{cr} results and the corresponding model predictions obtained from the literature.

B. Experimental Study

The preliminary study provides a clear understanding on the variations of time predictions based on the factors that are being considered. Based on the existing comparisons, one prediction model is selected for a verification purpose [15], and the model can be found from (1) as follows:

$$T_{cr} = \frac{377204.7\left(1+K\frac{C}{D}\right)\times\left\{\delta_0+P_{corr}R_0\frac{1}{E_{eff}}\left[\frac{(R_0+C)^2+R_0^2}{(R_0+C)^2-R_0^2}+V_c\right]\right\}}{\left(1-0.0055\frac{C}{D}\right)i_{corr}} \quad (1)$$

where T_{cr} is the time to crack the concrete [years], K is the short/long term factor (0.1~0.4), C is the cover depth of the

RC member [mm], D is the bar diameter [mm], δ_0 is the thickness of porous zone [mm], P_{corr} is the critical pressure on the concrete [MPa], R_0 is $\left(\frac{D}{2}+\delta_0\right)$ [mm], E_{eff} is the elastic modulus of the concrete [MPa], V_c is the Poisson's ratio, and i_{corr} is the corrosion rate [mm/year] or [μA/cm^2]. The porous zone thickness δ_0 is characteristically about 10-20 μm [25].

TABLE I
COMPARISON OF EXPERIMENTAL DATA AND MODEL PREDICTIONS

Reference	Cover (mm)	Corrosion Rate (μA/cm^2)	T_{cr} (Experi-mental) (Hours)	T_{cr} (Model prediction related to Reference No.) (Hours)				
				[3]	[16]	[14]	[15]	[12]
[3]	20	100	113	**145**	106	113	96	114
	50	100	208	**245**	174	140	166	96
	70	100	264	**251**	220	132	223	45
	70	10	2643	**2510**	2200	1320	2234	952
[16]	30	150	95	202	**90**	89	83	57
	30	100	147.5	192	66	**127**	113	81
[14]	30	150	91	197	46	**89**	75	56
	20	100	112	146	62	**113**	93	69
[15]	-	-	-	-	-	-	-	-
	30	3.75	0.72*	2.5*	0.2*	0.4*	0.6*	**0.6***
[12]	50	2.41	1.84*	1.3*	0.4*	0.7*	3.7*	**1.5***
	70	1.79	3.54*	2.3*	0.6*	1.2	4.0*	**3.3***

Note: The asterisk mark displays the time in years

The experimental program is designed to compare and verify the results with above selected model that are subjected to one-dimensional and two-dimensional chloride diffusion. Hence, the experimental study will be conducted for slabs and columns to represent aforementioned respective chloride diffusivities. The chloride diffusion can be accelerated by impressed current [8].

The slab elements are of 500 mm by 500 mm in size, and the columns are of 250 mm by 250 mm by 500 mm in size. The slab thickness varies depending on the cover depth that is being used. In this experimental design, two cover depths are used; 25 mm and 50 mm. Moreover, two different bar diameters are used for this study with 12 mm (column samples) and 16 mm (slab samples with single layer) rebars. Figs. 1 and 2 show the test setup as follows:



Fig. 1 Accelerated corrosion apparatus for slab elements

As shown in Figs. 1 and 2, both sample types are partially submerged in a 5% (w/w) sodium chloride (NaCl) solution. A potential gradient is supplied through an anode and a cathode by a power supply [29], [17]. Reinforcement of each structural element acts as the anodes, whereas the stainless steel acts as the cathode. The charge of the chlorides in the NaCl solution is negative; they are attracted by the anode which is connected to the reinforcement in each test setup. Due to the chloride migration based on either one-dimensional diffusion or two-dimensional diffusion, the passivation layer will be depleted, and the onset corrosion is taken place. Once the corrosion initiation is started, its mechanism will continue to propagate until cracking, and spalling of concrete cover is eventually observed [26]. The test setups are kept under a constant current at 2A until first sight of significant crack widths is to be seen. The minimum crack widths are observed continuously using a crack width gauge at 0.4 mm (0.016 in.) as this is the limit that ACI 224R-01 [1] allows for the crack control in RC structures.

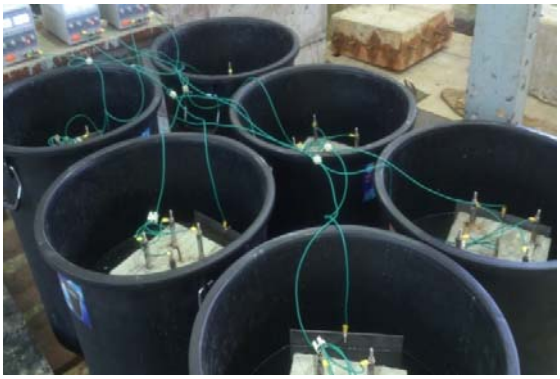


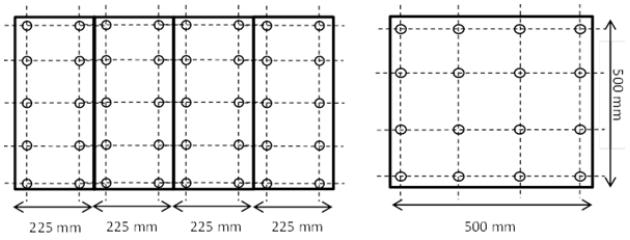
Fig. 2 Accelerated corrosion apparatus for column elements

C. Half-Cell Potential Readings at Cracking Stage

The half-cell potential is a probability indication of onset corrosion [29]. Higher potential reflects a higher probability of corrosion or mass loss around the half-cell sponge. Fig. 3 shows the locations where the half-cell potential readings are obtained at the stage of final cracking of both the samples.

Open Science Index, Civil and Environmental Engineering Vol:11, No:9, 2017 publications.waset.org/10007834/pdf

Open Science Index, Civil and Environmental Engineering Vol:11, No:9, 2017 publications.waset.org/10007834/pdf



(a) (b)

Fig. 3 Locations of half-cell potential readings (a) total outer surface of column (b) total outer surface of slab

D. Mass Loss Calculations

Once the reinforcements have undergone average expected crack widths as mentioned above, the samples will be demolished to evaluate the mass loss for the corrosion rate measurements. Cleaning procedures for corroded rebars are conducted based on the recommendations of "ASTM G1 standard practice for preparing, cleaning, and evaluation corrosion test specimens under chemical cleaning method" [30]. Cleaned rebars have lower cross sectional area due to the loss of mass from corrosion as shown in Fig. 4.



Fig. 4 Cleaned rebars after corrosion

The mass loss percentage can be determined by (2):

$$Mass\ loss\ percentage = \frac{m_i - m_f}{m_i} \times 100\ \% \qquad (2)$$

where m_i is the initial weight of each rebar before casting, and m_f is the final weight of each rebar after corrosion. The numerator indicates the mass loss occurred during corrosion process. This information is used to relate to the induced corrosion rate based on the guidelines provided by the ASTM G1 provisions as shown in (3):

$$i_{corr}\left(\frac{mm}{year}\right) = \frac{8.76\times10^4 \times Mass\ Loss(g)}{Area(cm^2)\times Density\left(\frac{g}{cm^3}\right)\times Time(hours)} \qquad (3)$$

E. Main Factors Controlling T_{cr}

During the preliminary stage, a significant number of prediction models are studied. Each of them differed from various factors that are accounted for in the T_{cr}. A Minitab analysis is used in order to see the fluctuation of these effects on the T_{cr}. It can capture the main effects that govern the T_{cr}. Under this analysis, Pareto charts, main effect plots, and contour plots are incorporated to visualize the fluctuation of effects on T_{cr}.

III. Results and Analysis

A. Verification of Model Compared to Experimental Results

The results are obtained for the one-dimensional diffusion (slab elements) and the two-dimensional elements (column elements) separately. The predicted time given in (1) is treated as a lower bound and an upper bound based on the critical pressure (P_{corr}) definitions [15], [28]. Hence, this model can predict a specific range for T_{cr} values. The lower bound tends to govern the partly cracked elastic behavior in concrete whereas the upper bound tends to govern the plastic behavior in concrete while cracking [24]. The upper bound and lower bound values are given in (4) and (5), respectively:

$$P_{corr} = \frac{2Cf_{ct}}{D} \qquad [Upper\ Bound\ P_{corr}] \quad (4)$$

$$P_{corr} = 0.6\left(0.5 + \frac{C}{D}\right) f_{ct} \qquad [Lower\ Bound\ P_{corr}] \quad (5)$$

where P_{corr} is the critical pressure due to corrosion expansion (MPa), C is the cover depth (mm), f_{ct} is the tensile strength of the concrete (MPa), and D is the bar diameter (mm). Following the figures, Figs. 5 and 6 illustrate the results obtained for both test samples subjected to accelerated two-dimensional chloride diffusion and one-dimensional chloride diffusion, respectively.

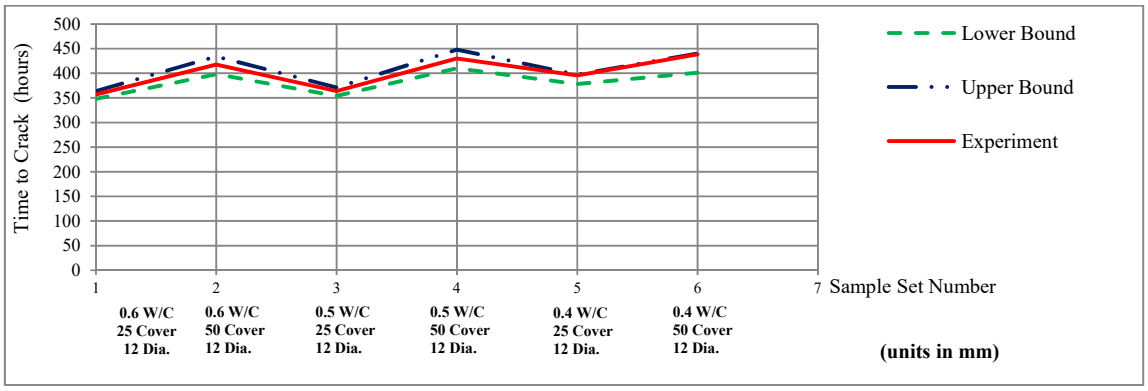


Fig. 5 Experimental results of T_{cr} for column elements

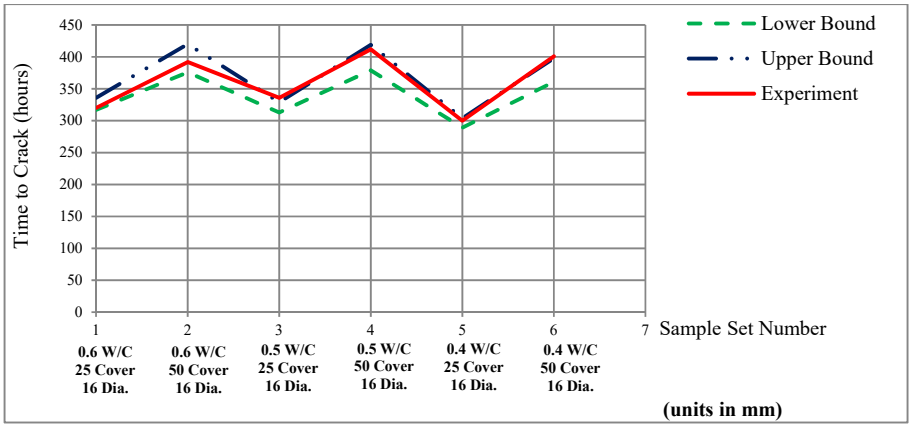


Fig. 6 Experimental results of T_{cr} for slab elements

The above figures show that the experimental data are in good terms with the predicted range of results based on the factors considered in the model. The obtained results are subjected to a comparison based on the accuracy of the model as shown in Figs. 7 and 8. It is found that the one-dimensional chloride diffusion accuracy varied ±20% compared to the perfect prediction case, whereas the two-dimensional chloride diffusion accuracy varied ±10% compared to the perfect prediction case. Hence, it is clear that the selected model is very subtle towards the behavior of the two-dimensional chloride diffusion.

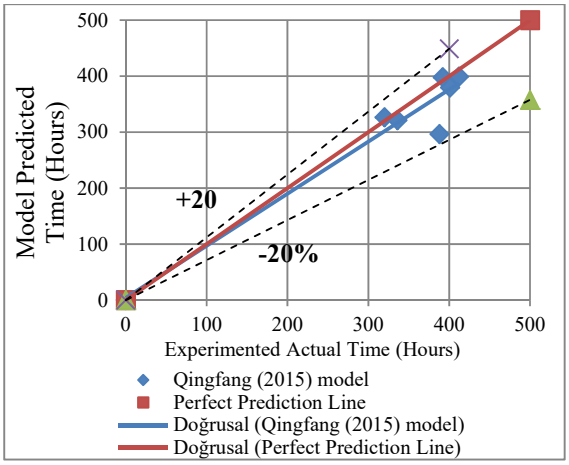


Fig. 7 Comparison of model prediction vs. actual time – slab elements (one-dimensional)

B. Half-Cell Potential

The half-cell potential readings are taken at each location as discussed in the above subsection C for both RC elements after corrosion cracks are observed at least 0.4 mm in width. The half-cell readings are higher at areas where higher amount of mass loss is occurred, and this is observed clearly with all the sample reinforcements after the demolition. All the samples showed that the amount of half-cell potential is proportional to the amount of mass loss occurred in a particular reinforcement. The variation of cover depths does not affect greatly due to the reason that the concrete has already cracked because of corrosion. Thus, the resistivity of the concrete cover has reduced significantly, and therefore the change in concrete cover depths has no effect at this stage. Examples of corrosion maps out of all 12 samples are shown in Figs. 9 and 10, and those corrosion maps depict the negative corrosion potential variation as in volts (V) before the demolition of the column sample and the slab sample, respectively. Further, it is observed that the amount of negative corrosion potential varied proportionally to the mass loss along each rebar.

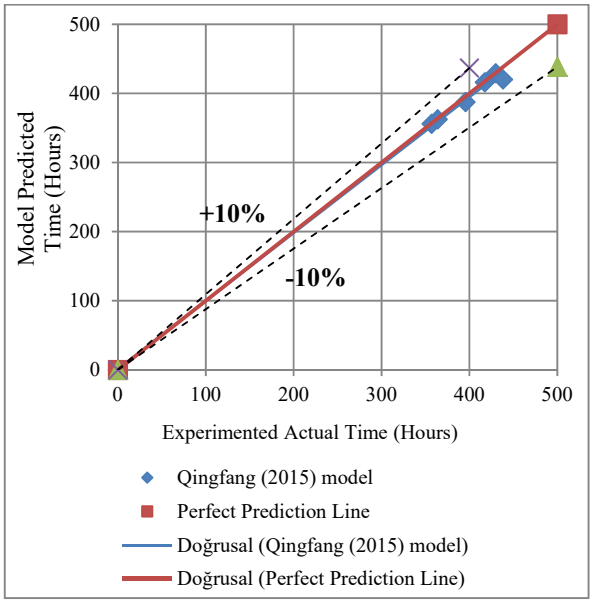


Fig. 8 Comparison of model prediction vs. actual time – column elements (two-dimensional)

C. Determination of Controlling Factor for T_{cr}

Three variables are used to study the significance of the influential factors that affects the T_{cr} namely; w/c ratio, bar diameter, and the concrete cover depth. Based on the T_{cr} values obtained from the experimental results, a statistical analysis is performed with predetermined lower bound and upper bound factors. Table II shows the lower bound and the upper bound factors that are included in the analysis.

Open Science Index, Civil and Environmental Engineering Vol:11, No:9, 2017 publications.waset.org/10007834/pdf

Open Science Index, Civil and Environmental Engineering Vol:11, No:9, 2017 publications.waset.org/10007834/pdf

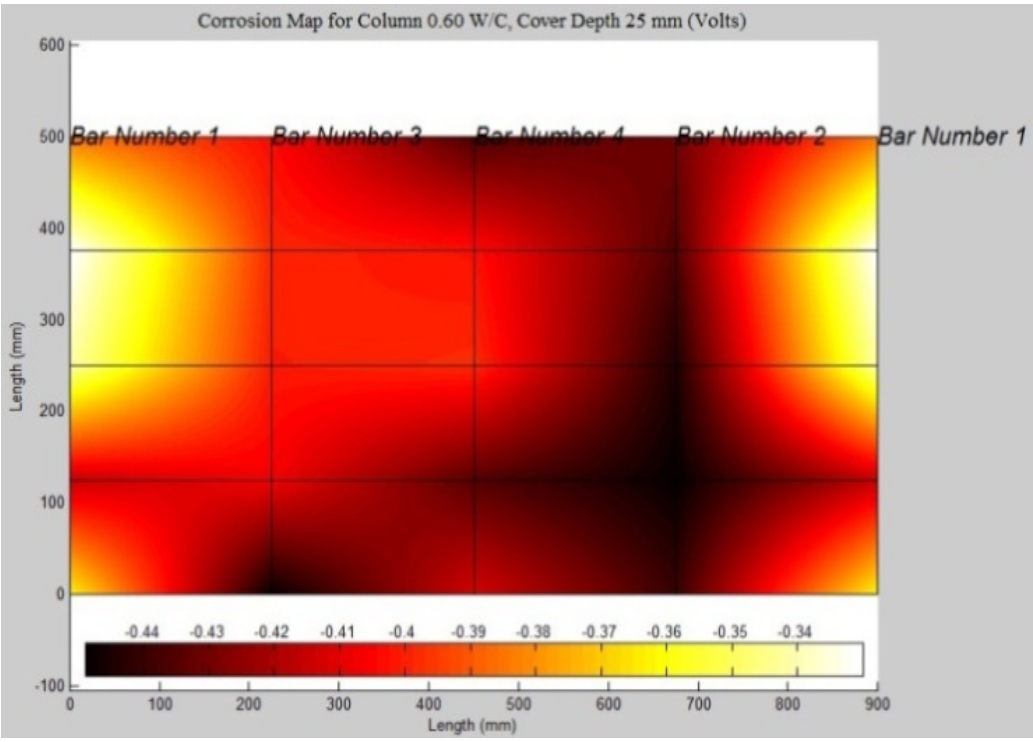


Fig. 9 Corrosion map – column surface along the rebars

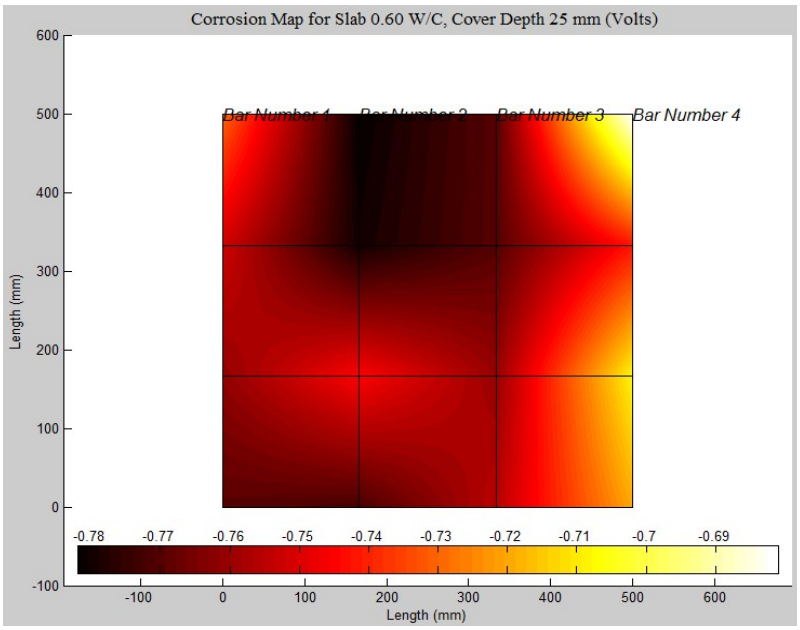


Fig. 10 Corrosion map – slab surface along the rebars

TABLE II
SELECTED FACTORS AND CORRESPONDING LOWER BOUNDS AND UPPER BOUNDS

Factors	Lower Bound	Upper Bound
W/C ratio	0.40	0.60
Bar Diameter	12 mm	16 mm
Concrete Cover Depth	25 mm	50 mm

The analysis is conducted via Minitab software, and it concluded that the governing factor that controls the T_{cr} due to corrosion is the cover depth. The following Pareto chart in Fig. 11 depicts that a higher effect is being contributed to the T_{cr} from concrete cover depth. However, other factors are found to be minimal in terms of affecting the T_{cr}. Further, from Fig. 12, it is seen that the cover depth has a significant influence on the T_{cr} in the contour plots generated by this statistical analysis. By and large, it can be concluded that the life span can be increased by using greater cover depths in the RC structures.

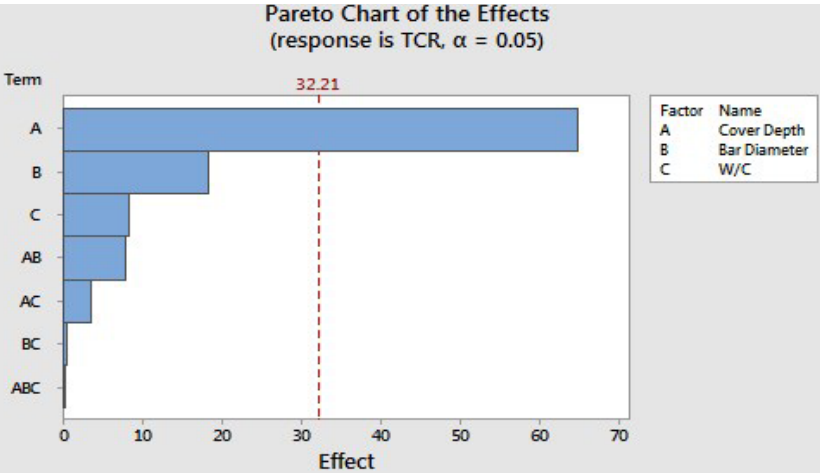


Fig. 11 Effects of factors on T_{cr}

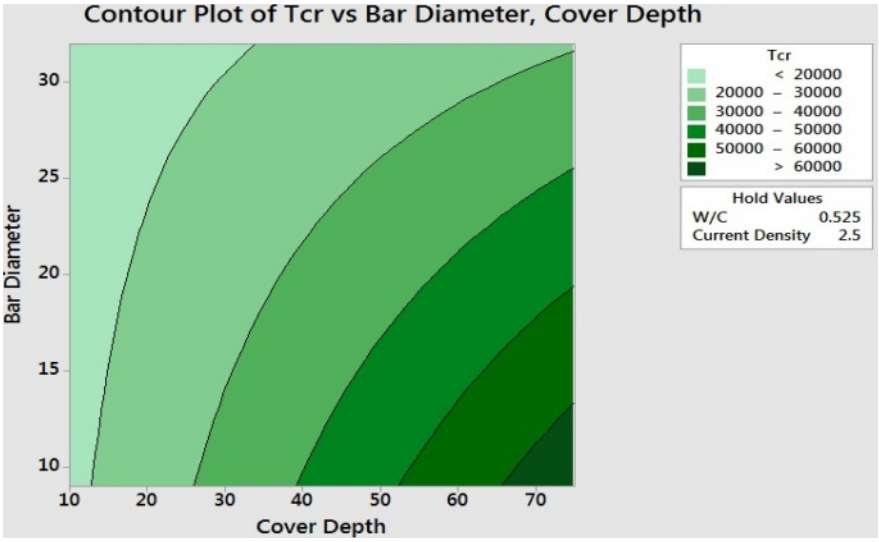


Fig. 12 Contour plot of T_{cr} of bar diameter (mm) and cover depth (mm)

IV. Practical Application

Several useful practical applications are identified from this research based on the results obtained in different points of views. Such practical applications can be utilized for existing buildings as well as for the future structures. As far as the existing buildings are concerned, the model that is used in this study can be an excellent tool to determine how much of time it would take to create corrosion cracks, and thereby, it can assess the present condition of the RC structure or member. Moreover, the half-cell potential values can detect where higher negative potentials exist along the structural member, and any localized repairing can be performed initially. And additionally, cover depth is the most influential parameter that controls the T_{cr}, and the future structures can be protected by providing higher cover depths so that it can enhance the resistance of the concrete to corrosion.

V. Conclusions

The selected model has a good correlation compared to the experimental study. Based on the results obtained from this study, the following conclusions are drawn.

1. The experimental results have shown that the selected model for both one-dimensional and two-dimensional chloride exposures had ±20% and ±10% respective accuracies compared to the experimental output. This makes the model quite sensitive for the two-dimensional chloride diffusion.
2. The model fits in between the lower bound and the upper bound for both the chloride diffusivity cases demonstrated in the experimental study.
3. Negative half-cell potential readings are proportional to the location where the amount of mass loss occurred during corrosion.
4. It is found that the cover depth has a significant effect on the T_{cr} and it helps to control the durability of the structures quite substantially.

Acknowledgment

The author acknowledges the greatest support and the funding provided by the school of Structural Engineering and

Open Science Index, Civil and Environmental Engineering Vol:11, No:9, 2017 publications.waset.org/10007834/pdf

Technology (SET) at Asian Institute of Technology (AIT), Thailand. His sincere appreciation goes to the committee at AIT for all the hard work and proper guidance to make this research work successful.

REFERENCES

[1] A. Abou-Zeid, J.H. Allen, J.P. Barlow, K. Carlson, G.T. Halvorsen, M.N. Hassoun, P. Hedli, T.C. Liu, Control of Cracking in Concrete Structures, 2001.
[2] S. A. Alghamdi, S. Ahmad, Service Life Prediction of RC Structures Based on Correlation between Electrochemical and Gravimetric Reinforcement Corrosion Rates, Cem. Concr. Compos. (2013) 64–68.
[3] C. Alonso, C. Andrade, J. Rodreguez, J. Diez, Factors Controlling Cracking of Concrete Affected by Reinforcement Corrosion, Mater. Struct. (1998) 435–441.
[4] Z. Bažant, L. Estenssoro, Surface Singularity and Crack Propagation. International Journal of Solids and Structures, Int. J. Solids Struct. (1979) 405–426.
[5] H. J. Dagher, S. Kulendran, Finite Element Modeling of Corrosion Damage in Concrete Structures, ACI Struct. J. (1992) 699–708.
[6] T. Hoar, The Production and Breakdown of the Passivity of Metals, Corros. Sci. (1967) 341–355.
[7] M. Ja, Kolotyrkin, Effects on Anions on the Dissolution Kinetics of Metals, J. Electrochem. Soc. (1961) 209–216.
[8] A. Jamali, U. Angst, B. Adey, B. Elsener, Modeling of Corrosion-Induced Concrete Cover Cracking, Constr. Build. Mater. (2013) 225–237.
[9] M. Lacasse, D. Vanier, Durability of Building Materials and Components, Duracrete. (1999) 1343–1356.
[10] H. P. Leckie, H. Uhlig, Environmental Factors Affecting the Critical Potential for Pitting in 18-8 Stainless Steel, J. Electrochem. Soc. (1966) 1262–1267.
[11] L. F. Lin, C. Y. Chao, D. D. Macdonald, A Point Defect Model for Anodic Passive Films - II, J. Electrochem. Soc. (1981) 1194–1198.
[12] Y. Liu, Modeling the Time to Corrosion Cracking of the Cover Concrete in Chloride Contaminated Reinforced Concrete Structures, Blacksburg, VA, 1996.
[13] Y. Liu, R. Weyers, Modeling the Time to Corrosion Cracking of the Cover Concrete in Chloride Contaminated Reinforced Concrete Structures, Blacksburg, VA, 1998.
[14] C. Lu, W. Jin, R. Liu, Reinforcement Corrosion-Induced Cover Cracking and its Time Prediction for Reinforced Concrete Structures, Corros. Sci. (2011) 1337–1347.
[15] Q. Lv, R. Zhu, Model for Forcasting the Time of Corrosion-Induced Reinforced Concrete Cracking, in: Int. Conf. Performance-Based Life-Cycle Struct. Eng., Brisbane Convention and Exhibition Centre, Brisbane, Australia, 2015: p. ID210.
[16] T. Maaddawy, K. Soudhki, A Model for Prediction of Time from Corrosion Initiation to Corrosion Cracking, Cem. Concr. Compos. (2007) 168–175.
[17] P. McGrath, R. Hooton, Effect of Binder Composition on Chloride Penetration Resistance of Concrete, in: American Concrete Institute, Detroit, MI, 1997.
[18] P. K. Mehta, No Title, in: S. W. Tonini, D. E., Dean (Ed.), Eff. Cem. Compos. Corros. Reinf. Steel Concr., ASTM, Baltimore, MD, 1977: pp. 12–19.
[19] F. J. Molina, C. Alonso, C. Andrade, Cover Cracking as a Function of Rebar Corrosion: Part 2 - Numerical Model, Mater. Struct. (1993) 532–548.
[20] S. Morinaga, Prediction of Service Lives of Reinforced Concrete Buildings based on Rate of Corrosion in Reinforcing Steel, (1988).
[21] S. Morinaga, Prediction of service lives of reinforced concrete buildings based on corrosion rate of reinforcing steel, in: Proc. Fifth Int. Conf. Durab. Build. Mater. Components, E. & F.N. SPON, London, UK, 1990: pp. 5–16.
[22] A. Muñoz, C. Andrade, Reinforced Concrete Cover Cracking due to the Pressure of Corrosion Products, Adv. Constr. Mater. (2007).
[23] N. Sato, Anodic Breakdown of Passive Films on Metals, J. Electrochem. Soc. (1982) 255–260.
[24] R. Tepfers, Cracking of Concrete Cover along Anchored Deformed Reinforcing Bars, Mag. Concr. Res. (1979) 3–12.
[25] P. Thoft-Christensen, Stochastic modelling of the crack initiation time for reinforced concrete structures, ASCE Struct. Congr. (2000) 8.
[26] K. Tuutti, Corrosion of Steel in Concrete, Swedish Cement and Concrete Research Institute, 1982.
[27] K. Yokozeki, K. Motohashi, K. Okada, T. Tsutsumi, A Rational Model to Predict the Service Life of RC Structures in Marine Environment, ACI. (1997) 777–799.
[28] Y. Zhao, W. Jin, Modeling the Amount of Steel Corrosion at the Cracking of Concrete Cover, Adv. Struct. Eng. (2006) 687–696.
[29] ASTM C876 Standard Test Method for Half-Cell Potentials of Uncoated Reinforcing Steel in Concrete, (1999).
[30] ASTM G1 Standard practice for preparing, cleaning, and evaluation corrosion test specimens under chemical cleaning method, 1999.

Open Science Index, Civil and Environmental Engineering Vol:11, No:9, 2017 publications.waset.org/10007834/pdf